



Cite this: *Anal. Methods*, 2024, **16**, 2625

Received 16th February 2024  
 Accepted 15th April 2024

DOI: 10.1039/d4ay00278d

[rsc.li/methods](https://rsc.li/methods)

# Electroanalysis overview: additive manufactured biosensors using fused filament fabrication

Robert D. Crapnell  and Craig E. Banks  \*

Additive manufacturing (3D-printing), in particular fused filament fabrication, presents a potential paradigm shift in the way electrochemical based biosensing platforms are produced, giving rise to a new generation of personalized and on-demand biosensors. The use of additive manufactured biosensors is unparalleled giving rise to unique customization, facile miniaturization, ease of use, economical but yet, still providing sensitive and selective approaches towards the target analyte. In this mini review, we focus on the use of fused filament fabrication additive manufacturing technology alongside different biosensing approaches that exclusively use antibodies, enzymes and associated biosensing materials (mediators) providing an up-to-date overview with future considerations to expand the additive manufacturing biosensors field.

## 1. Introduction

Additive manufacturing (3D-printing) is a revolutionary technology that allows the user to build 3-dimensional objects through a computer-aided design (CAD) file. The file is converted for the additive manufacturing technology of choice through a process called slicing, which produces a .GCODE file and acts as instructions for the printer. In the case of Fused Filament Fabrication (FFF, commonly referred to as Fused Deposition Modelling or FDM), this file instructs the printer to extrude loaded thermoplastic filaments into the CAD design, layer by layer.<sup>1–10</sup> The cost of additive manufacturing technology has reduced over the years where one can easily buy a reliable, robust but yet, high-performance FFF printer for under 500 GBP which greatly extends the use within academic and industrial research groups. FFF has significant advantages such as: short lead times, low cost production runs, low waste production in comparison to subtractive manufacturing approaches, the ability to produce complex geometries which can be customized and can provide on-site manufacturing *via* global connectivity.<sup>11</sup> Due to the availability of conductive filament for FFF it has an advantage over many other additive manufacturing techniques for the production of electrodes. As such, there has been a huge rise in the amount of publications using FFF for the production of working electrodes for electrochemical applications.

Electrochemistry is a core fundamental science which is concerned with electron transfer and supports energy storage, such as batteries and supercapacitors, energy transformation including fuel cells and solar cells, electroanalysis including forensic and environmental applications, and most importantly for this review, biosensors, which is the application of

electrochemical processes to measure the quantity of a biologically relevant target analyte. The field of electrochemical biosensors is diverse, tackling environmental monitoring, medical diagnosis, athletic performance tracking *via* wearable biosensors and food and drink safety.<sup>12–24</sup> The design and fabrication of electrochemical biosensors involves customization of sensor substrates, selection, and integration of a biorecognition element specific to the target analyte along with a transduction platform to detect the biorecognition event and convert it to a recordable form. It is this requirement for a conductive transduction platform which leads to FFF and electrochemistry synergising so well, coined additive manufacturing electrochemistry. Electrochemical based biosensors have materialized as a favourable point-of-care approach for the immediate and rapid detection of target analytes. These electrochemical biosensors offer various advantages, such as *in situ* analysis, minimal sample preparation requirements, low-cost instrumentation, rapid analysis times, cost efficiency, facile miniaturization, yet, provide selectivity and sensitivity towards the target analyte.

The use of additive manufacturing with electrochemistry has a promising future, termed: additive manufacturing electrochemistry.<sup>11</sup> Additive manufacturing electrochemistry utilizes the ability to use electrically conductive filaments which can be rapidly printed out on FFF technology allowing diverse electrode materials and devices to be realized. There are two types of publication in this area, the first that utilizes commercially available filaments,<sup>25–30</sup> for example. Typically these are comprised of plastic poly(lactic acid) (PLA, >65 wt%) as the bulk material, an unidentified polymer (<12.7 wt%) and nanocarbon black (CB, <21.43 wt%) acting as the conductive filler,<sup>11</sup> and PLA with graphene (~13 wt%),<sup>31</sup> but these are limited in terms of their composition, functionalities and conductivities, with the most commonly used commercial product producing

Faculty of Science and Engineering, Manchester Metropolitan University, Chester Street, Manchester M1 5GD, UK. E-mail: [c.banks@mmu.ac.uk](mailto:c.banks@mmu.ac.uk)





**Table 1** An overview of approaches where fused filament fabrication has been utilised for the creation of working electrodes in electrochemical biosensors, detailing the electrode material, analyte detected, linear range, limit of detection, the sample medium and whether the filament was commercial or bespoke<sup>a</sup>

Electrode	Analyte	Linear range	Limit of detection	Sample medium	Filament type	Reference
PLA, CB	Glucose	2–28 mM	—	—	Commercially available filament	43
PLA, graphene	1-Naphthol	3–100 $\mu\text{M}$	—	—	Commercially available filament	44
PLA, graphene	Glucose	0.5–6.3 mM	15 $\mu\text{M}$	Plasma from bovine	Commercially available filament	45
PLA, graphene	Catechol	30–700 $\mu\text{M}$	0.26 $\mu\text{M}$	Natural water	Commercially available filament	46
PLA, graphene	Hydrogen peroxide	25–100 $\mu\text{M}$	9.1 $\mu\text{M}$	Human serum	Commercially available filament	47
PLA, graphene	COVID-19 protein	1–10 $\mu\text{g mL}^{-1}$	0.5 $\mu\text{g mL}^{-1}$	Human serum	Commercially available filament	48
PLA, CB	N protein, $\text{S}_{\text{RBD}}$ protein, and anti- $\text{S}_{\text{RBD}}$	1–100 $\text{pg mL}^{-1}$	5, 1 and 0.1 $\text{pg mL}^{-1}$	Saliva and human serum	Commercially available filament	49
PLA, CB	Cholesterol and choline	30–240 $\mu\text{M}$ ; 0.5–4 $\mu\text{M}$	3.36 $\mu\text{M}$ ; 0.08 $\mu\text{M}$	Artificial blood	Commercially available filament	50
PLA, graphene	Glucose	500 $\mu\text{M}$ –10 mM	158 $\mu\text{M}$	Apple cider	Commercially available filament	51
PLA, CB	<i>Hantavirus araucaria</i> nucleoprotein	30–240 $\mu\text{g mL}^{-1}$	22 $\mu\text{g mL}^{-1}$	Human serum	Commercially available filament	52
PLA, graphene	cDNA of SARS-CoV-2	1–50 $\mu\text{M}$	0.3 $\mu\text{M}$	Synthetic saliva and human serum	Commercially available filament	53
PLA, CB	<i>Salmonella typhimurium</i>	$10^1$ – $5 \times 10^6$ cfu $\text{mL}^{-1}$	5 cfu $\text{mL}^{-1}$	Chicken broth and chicken rinse	Commercially available filament	54
PLA, graphene	1-Naphthyl phosphate	2.5–50 $\mu\text{g mL}^{-1}$	0.95 $\mu\text{g mL}^{-1}$	—	Commercially available filament	55
PLA, graphene	Extracellular matrix biomarker: Fibronectin	0.1–10 $\mu\text{g mL}^{-1}$	—	Breast cancer cells (CAL51)	Commercially available filament	56
PLA, graphene	PARK7/DJ-1 protein	5–200 $\mu\text{g L}^{-1}$	1.01 $\mu\text{g L}^{-1}$	Human blood serum and synthetic cerebrospinal fluid	Commercially available filament	57
PLA, CB	Glucose	1–100 mM	—	HepG2 cells in 3D hydrogels	Commercially available filament	58
PLA (60 wt%) graphite (40 wt%)	SARS-CoV-2 spike S1 protein	5–75 nM	1.36 nM	Synthetic saliva	Bespoke filament	36
PLA (71.5 wt%), CB (28.5 wt%) rPLA (65 wt%), PES (10 wt%), CB (15 wt%), COOH-MWCNTs (10 wt%) PLA (71.5 wt%), CB (28.5 wt%)	Hydrogen peroxide Yellow fever virus cDNA SARS-CoV-2 spike S1 protein	5–350 $\mu\text{M}$ 0.5–15 $\mu\text{M}$ 0.01–4.5 nM	1.03 $\mu\text{M}$ 0.138 $\mu\text{M}$ 2.7 pM	Milk Human blood serum Human serum and synthetic saliva	Bespoke filament Bespoke filament Bespoke filament	59 60 61

<sup>a</sup> Key: PLA: poly(lactic acid); rPLA: recycled poly(lactic acid); PES: polyethylene succinate; CB: carbon black; MWCNTs: multi-walled carbon nanotubes.

a resistance of  $\sim 2\text{--}3\text{ k}\Omega$  across 10 cm of filament. The second type of publication involves the production of bespoke conductive filaments, where different types of plastic can be employed, preferably from recycled sources, a range and mixture of conductive nanoparticles can be used, and biodegradable and sustainable plasticizers can be utilized. These all aim to improve the electrochemical and printing performance over that achievable using commercially available filaments, with many easily printable materials offering significantly lower resistances ( $200\text{--}900\text{ }\Omega$  over 10 cm of filament length).<sup>32–38</sup>

In this minireview, we focus upon the use of FFF additive manufacturing technology along with the use of biosensors that are exclusively using antibodies, enzymes and associated biosensing materials (mediators). This minireview paper looks to provide an overview of the literature on the use of additive manufacturing for the production of electrochemical biosensors, with the focus on fused filament fabrication for the production of the electrode and offer some suggestions for how this field can progress in the future. If one searches the literature using the terms “additive manufacturing” and “biosensors”, over of 400 papers will result, but on closer inspection, these are using different additive manufacturing technology (we focus solely on FFF) and furthermore, these are used in the fabrication of holders/cells *etc.* rather than the working electrode used within biosensors. For overviews on how more additive manufacturing techniques have been used to aid the development of electrochemical biosensing platforms we direct the reader to other reviews.<sup>39–41</sup> We note that Molecularly Imprinted Polymers (MIPs) have been used in conjunction with electrochemistry for similar targets,<sup>42</sup> but as there are no examples within additive manufacturing electrochemistry and they don't meet the strict definition of biosensors, they have been omitted. As can be observed within inspection of Table 1, we have divided up the literature into additive manufacturing biosensors using commercially available filaments and those reporting the development of bespoke filaments for additive manufacturing biosensors, noting that these are placed in chronological order. Within Table 1, we can see that each electrode is reported through its composition, which analyte has been determined, the linear range and limit of detection (LoD) achieved, and the real sample medium used for proof-of-concept. In the first section, we summarize the approach of using commercially available filament for additive manufacturing biosensors.

## 2. Additive manufacturing biosensors using commercially available filaments

One of the earliest approaches using additive manufacturing for the production of an electrochemical biosensor was reported by Katseli and co-workers<sup>43</sup> who used a commercial filament comprised of nanocarbon black within PLA. They used this alongside non-conductive PLA within a 3D printer with two extruder heads; see Fig. 1A. In their proof-of-concept approach they made an integrated device which, as shown within Fig. 1B, shows circular electrodes that comprise the working, counter

and pseudo-reference electrodes and are held with a non-conductive PLA holder. It is reported that these can be fabricated within 9 minutes. The authors modified the electrode by immersing it into a solution comprising Nafion® and glucose oxidase ( $\text{GO}_x$ ) enzyme. In such an approach, which utilized first generation glucose biosensor technology,<sup>62</sup> the enzymatic conversion of glucose by  $\text{GO}_x$  generates hydrogen peroxide. The production of hydrogen peroxide can then be measured *via* a chronoamperometric measurement. This gave rise to a linear range between 2 to 28 mM of glucose, suggesting that this technology has potential use for glucose determination within real samples.<sup>43</sup> Dual extruder FFF has been taken further to print the electrodes and electrochemical cell all within a single print,<sup>63</sup> although not for biosensing this device provides an example as to how the facile production of a biosensor device within a single print could be achieved. This facile production would be a huge step toward commercialisation of additive manufactured electrochemical biosensors. This print was also shown to be recyclable,<sup>64</sup> which indicates another area of benefit for additive manufacturing electrochemistry over more established techniques such as screen-printing. The sensing of glucose is a key biosensor target and has continued to be the focus of immense research activity where continuous glucose monitoring can reduce the risks of diabetes induced diseases allowing the diabetics to sustain a healthy lifestyle while precluding the costly and lethal late-stage diabetic complications.<sup>65</sup>

To this end, Lee *et al.*<sup>58</sup> report on the development of an organ-on-a-chip system that mimics the tissue microenvironment to senses glucose; see Fig. 1C. This provides an overview of how they fabricated their liver-on-a-chip device which uses a liver *in vitro* model by additive manufacturing using hepatocellular carcinoma (HepG2) as the cell source.<sup>58</sup> The authors report the use of conductive (nanocarbon black) and nonconductive filaments to construct an integration sensor and chip approach. The authors constructed their glucose biosensor by mixing  $\text{GO}_x$  with Nafion® alongside multi-walled carbon nanotubes (MWCNTs), which are then drop-cast onto the working electrode. This glucose sensor exhibited a linear range over 1–100 mM which encompasses the general blood sugar levels of 2–40 mM. The authors then demonstrated that they could measure glucose within HepG2 cells, providing a liver *in vitro* model where additive manufacturing has allowed the development a portable, economical glucose monitoring device. Others have followed the trend where they change their nanocarbon commercially available filament to a graphene based commercial one, as reported by Cardoso and co-workers.<sup>45</sup> They printed their working electrode and polished with sandpaper before immersing in dimethylformamide (DMF) for 10 min, which erodes the PLA that covers the active graphene material giving rise to a beneficial electrochemical response due to the increased number of triple-phase boundaries. In the authors approach, they used  $\text{GO}_x$  with glutaraldehyde adopting a “second” generation glucose biosensor.<sup>62</sup> This involves two steps: first, flavin adenine dinucleotide (FAD), the active centre of the enzyme acts as an electron mediator for glucose oxidation to glucolactone and reduces to flavin adenine dinucleotide



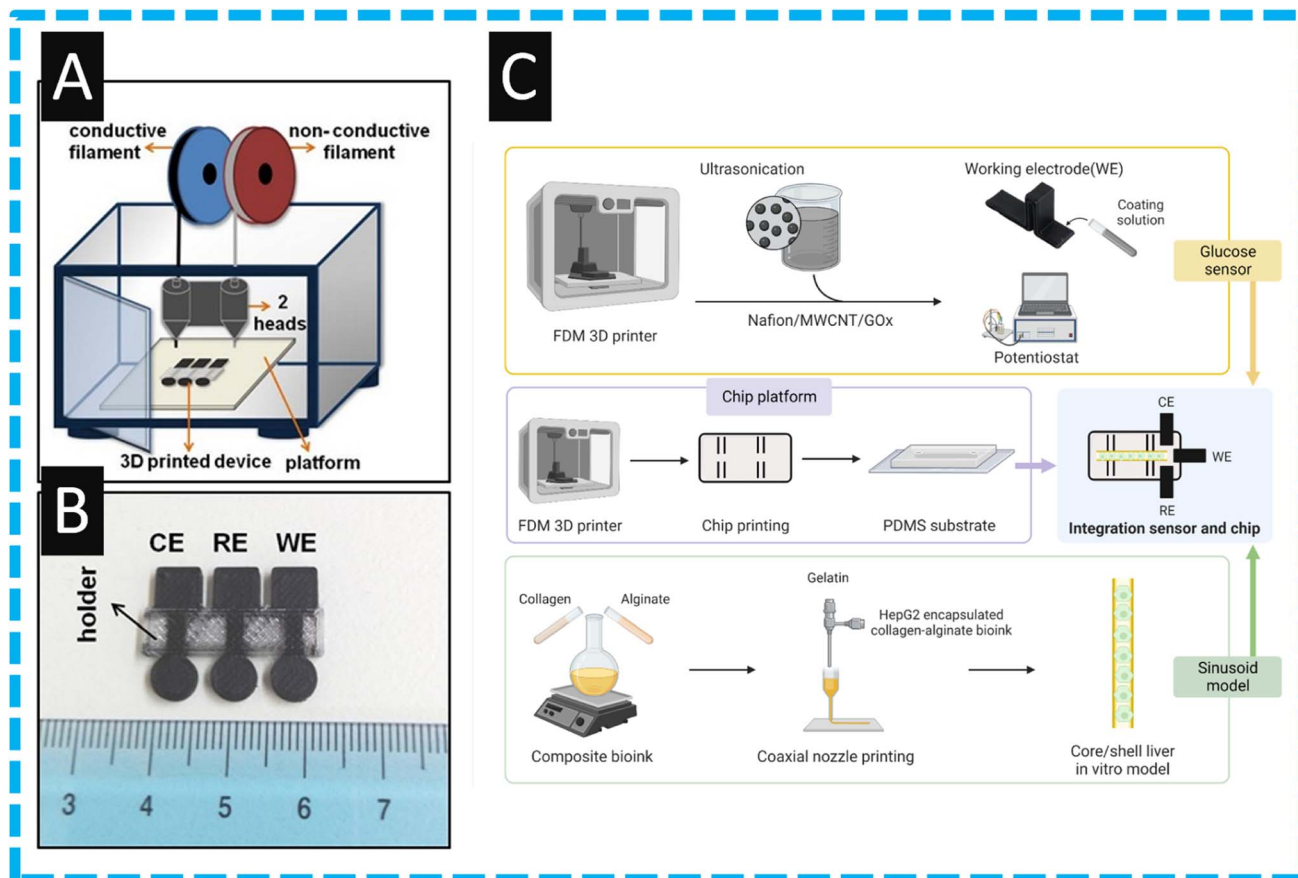


Fig. 1 (A): A schematic illustration of a fused filament fabrication printer with two print heads, (B) a photograph of the additive manufactured integrated device with the three electrodes printed from commercial conductive filament and the holder printed from commercial nonconductive filament. Figure reproduced from ref. 43. Copyright 2019 Elsevier. (C): Provides a summary of the integration process of glucose biosensor and liver-on-a-chip. The top row corresponds to the printing and then modification of the working electrode through drop casting. The second row illustrates the printing of the chip, and the third line represents the ink creation and printing for the *in vitro* model. Reproduced from ref. 58. Copyright 2023 Wiley.

(FADH<sub>2</sub>). In the second step, the FADH<sub>2</sub> is reverted again to FAD, and the electron involved in this oxidation is transferred to FCA, reducing Fe(III) to Fe(II). The use of glutaraldehyde allows for cross-linking with oxygenated functional groups present on the surface of the graphene with GO<sub>x</sub>. The authors demonstrated that the glucose sensor is linear over the range of 0.5–6.3 mM with a LoD of 15 μM, and then applied it to the determination of spiked plasma from bovine, producing a reported recovery value from 94–104%.<sup>45</sup> Last, the authors show the stability by relative standard deviation (RSD) values of 5.0 mM glucose detection, performed intra-day ( $n = 5$ ) and inter-day ( $n = 10$ ) with values of 3.7% and 4.2%, respectively. The use of graphene meant the presence of oxygenated groups on the electrode surface, which facilitated the modification through cross-linkage, resulting in high selectivity and stability for glucose measurements. Following such an approach reported above,<sup>45</sup> others have followed where they activated the electrode within DMF immersion to remove the insulating PLA polymer, followed by electrochemical treatment in order to generate carboxyl groups. These were reacted with *N*-(3-dimethylaminopropyl)-*N'*-ethylcarbodiimide hydrochloride (EDC) and *N*-

hydroxysuccinimide (NHS) to prepare a covalently modified electrode. This was tested and exhibited a linear range of 500 μM–10 mM with a LoD of 158 μM and was then applied to the determination within apple cider.<sup>51</sup>

Global health crises caused by coronavirus disease 2019 (COVID-2019) was instigated by a novel coronavirus known as Severe Acute Respiratory Syndrome Coronavirus 2 (SARS-CoV-2) and was identified as a pandemic by the World Health Organization (WHO) on March 11, 2020.<sup>48</sup> Electrochemical biosensors have emerged as promising alternatives in comparison to reverse transcription polymerase chain reaction (RT-PCR) assays, which were the primary method of identifying infection during the pandemic. As such, there are many reports on the design, fabrication and testing of COVID-19 electrochemical biosensors. For example, the use of electrode surface engineering has developed an additively manufactured biosensor for COVID-19 spike protein receptor binding domain (RBD) Coronavirus.<sup>48</sup> Shown within Fig. 2A is an overview of how the authors fabricated the biosensor. First, a lollipop electrode was additively manufactured and then then subjected to DMF immersion and electrochemical pretreatment. Next, the *in situ*



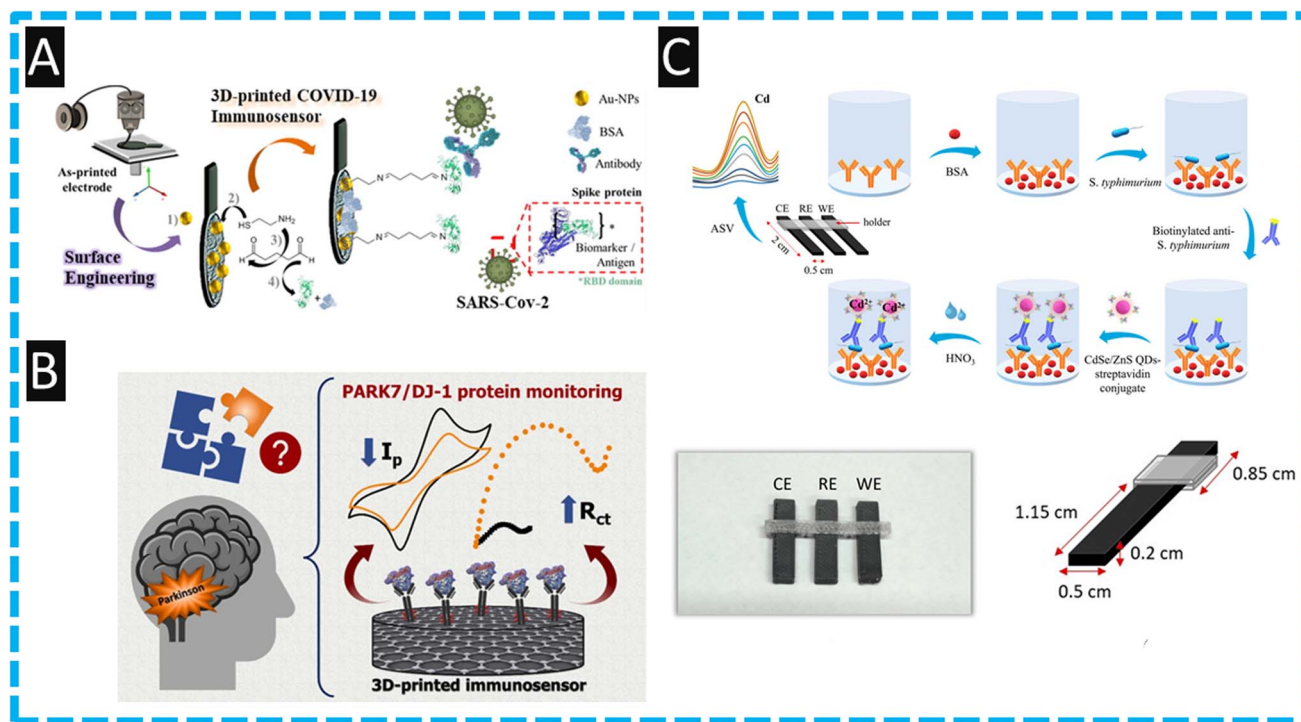


Fig. 2 (A): An overview of how the authors fabricated their COVID-19 sensor, starting with printing of the electrode, followed by deposition of gold nanoparticles and coupling of the antibodies. Figure reproduced from ref. 48. Copyright 2021 Elsevier. (B): A graphical overview of how PARK7/DJ-1 protein is measured providing information about Parkinson's disease, showing how the cyclic voltammetric signal decreases and the charge transfer resistance increases upon analyte binding. Figure reproduced from ref. 57. Copyright 2023 Elsevier. (C): Assembly schematic for the production of the immunoassay, photographs of the 3D printer electrodes and a schematic with dimensions of the electrodes used. Figure reprinted with permission under a Creative Commons attribution-type BY from ref. 54. Copyright 2023 MDPI.

incorporation of gold nanoparticles (AuNPs) onto the surface of the electrode, whereby the AuNPs are formed *via* an eco-friendly approach involving the electrostatic interaction between the surface oxygen groups on the carbon in the presence of gold(III) ions. Following this, the electrodes were immersed in 10 mM  $\text{NaBH}_4$  to induce zero valent gold metal. The immobilised gold nanoparticles are then used to form a functionalized electrode using cysteamine and crosslinking with glutaraldehyde. Last, the terminal aldehyde groups of the cross-linker are used for anchoring the antibody and finally, Bovine Serum Albumin (BSA) is added to remove NHS residual sites. This biosensor reports a LoD of  $0.5 \mu\text{g mL}^{-1}$  which was shown to be used within human serum. This report has opened the opportunity of using additive manufacturing technology for the eco-friendly production of biosensors, however whether a sensor with this many post-print manufacturing steps could realistically be produced at a low-cost on a large scale remains to be proven.

Kalinke and co-workers<sup>57</sup> have reported a additively manufactured immunosensor for the diagnosis of Parkinson's disease by measuring PARK7/DJ-1 protein within human blood serum and synthetic cerebrospinal fluid. Parkinson's disease is a neurodegenerative disease where DJ-1 protein, at low levels can be correlated to the dysregulation of the PARK7 gene expression. It is reported that the different stages of Parkinson's (I, II, III, or IV) have an average concentration of  $30 \mu\text{g L}^{-1}$ .<sup>66,67</sup> To produce their electrochemical sensor the authors first used

chemical and electrochemical activation, immersing the additively manufactured electrode in sodium hydroxide for 30 min followed by holding the electrode at a potential of +1.8 V for 900 seconds within a phosphate buffer (pH 7.4) which developed carboxyl groups upon the graphene surface. Second, the authors used EDC and NHS for the immobilization of the anti-PARK7/DJ-1 antibodies. Third, the authors used BSA to block NHS residual sites. The authors used two electrochemical methods of detection, firstly cyclic voltammetry in conjunction with the redox probe ferrocenemethanol, which in the presence of PARK7/DJ-1 protein, saw the anodic and cathodic peak currents decrease. Then using electro-chemical impedance spectroscopy, the charge-transfer resistance (RCT) increased with additions of PARK7/DJ-1 protein due to the antigen-antibody immunocomplex acting as a barrier, compromising the electron transfer and the analytical signal; see Fig. 2B. The authors demonstrated their immunoassay could measure PARK7/DJ-1 protein over the range of  $5\text{--}200 \mu\text{g L}^{-1}$  and a LoD of  $1.01 \mu\text{g L}^{-1}$ . The authors then applied this to the detection of PARK7/DJ-1 within human blood serum and synthetic cerebrospinal fluid by spiking the samples with 30, 40 and  $100 \mu\text{g L}^{-1}$ , which equated to normal to raised levels, observing good recovery values over the range of 94–104%.<sup>57</sup> This work is proof-of-concept and further work needs to be compared to the electrochemical measurement of PARK7/DJ-1 protein against standard clinic/laboratory measurements as a next stage.

Other uses of commercially available filaments have been directed into an immunosensor using CdSe/ZnS quantum dots to sense *Salmonella typhimurium*.<sup>54</sup> As shown within Fig. 2C, the use of FFF additive manufacturing has realized a fully integrated additive manufacturing device by using nanocarbon black embedded PLA as the conductive filament for electrode production and non-conductive PLA to print a holder. The sensor employed a sandwich type immunoassay using a biotinylated detection antibody to ensure that the binding of streptavidin conjugated to the CdSe/ZnS quantum dots (Fig. 2C). When the assay has completed, the quantum dots are dissolved within an acid media where the authors used differential pulse anodic stripping voltammetry to quantify the cadmium released;<sup>54</sup> the authors report a LoD of 5 cfu mL<sup>-1</sup>. It is interesting to note that for poultry product to be considered free of salmonella in EU countries, according to Regulation (EC) No 2073/2005, salmonella should not be detected in 25 g of the product. To verify the presence of salmonella, the authors used an accredited reference standard which allowed them to measure 1 cfu mL<sup>-1</sup> after a pre-enrichment of 5 h. This allowed the authors to indicate the presence of salmonella within Chicken broth and chicken rinse. This was compared to an agar plate that had been culturing for 24 h where the immunosensor developed could detect the presence of a single bacterium in the sample.<sup>54</sup> The authors state that the additively manufactured electrochemical immunosensor can potentially find wide applications in the food analysis sector for the sensitive and rapid detection of salmonella at the point-of-need. We note though that PLA shows significant ingress of solution within aqueous samples, including conductive PLA,<sup>68</sup> and therefore care must be used when using these electrodes or containers. They can only be used for a single sample, and there must be suitable recycling methodologies put in place to reduce the environmental impact of these devices.

Related to the above report,<sup>52</sup> detection of hantavirus Araucaria nucleoprotein is shown to be possible using nanocarbon with PLA filament which is electrochemically activated and using EDC/NHS reaction to immobilize antibodies. Hantavirus is a single-strained RNA virus, usually found hosted by rats or bats, but represents a higher threat of infection in humans. This commonly results in Hantavirus pulmonary syndrome in the Americas, and hemorrhagic fever with renal syndrome over the Eurasia region, with a lethality rate of around 40%, due to the lack of specific treatment.<sup>52,69</sup> This immunoassay gave a linear range from 30 to 240 µg mL<sup>-1</sup> with a LoD of 22 µg mL<sup>-1</sup> using cyclic voltammetry. The selectivity against VP2 protein from Gumboro disease was tested as it is a potential interferent due to a similar basic structure, where the authors show that using 600 µg mL<sup>-1</sup> there was no interference. The authors go on to show proof-of-concept for the immunoassay by measuring Hantavirus within human serum. This work has the potential to provide detection that can be useful of clinical treatment decisions. Additionally, additive manufacturing is unique in providing the ability to print sensors in the areas of most need through simply transferring the print file, thus avoiding hefty transportation costs. Other work has used graphene within PLA commercial filaments to produce a genosensor for the detection

of DNA hybridization.<sup>55</sup> In their approach, they modified their additively manufactured electrode with a target DNA. This was hybridized with a biotinylated DNA probe, allowing the binding of streptavidin-alkaline phosphatase conjugate. This was detected using enzymatic conversion of an electro-inactive compound, 1-naphthyl phosphate, into an electro-active indicator, 1-naphthol, to produce a signal. This genosensor was shown to respond to 1-naphthyl phosphate over the range of 2.5 to 50 µg mL<sup>-1</sup> with a LoD of 0.95 µg mL<sup>-1</sup>.<sup>55</sup>

The usefulness of additive manufacturing is exemplified through the report of an additively manufactured 4 electrode biochip for the simultaneous measurements of different biomarkers within a single assay.<sup>50</sup> Using a one-step approach by additive manufacturing a miniature vessel (200 µL) printed in a non-conductive PLA with four integrated electrodes printed from a nanocarbon PLA filament which comprises two working electrodes and alongside a reference and counter electrodes. One working electrode was modified with cholesterol oxidase, while the other with choline oxidase through adsorption onto which, Nafion® is applied. Through the use of a bipotentiostat, the working electrodes simultaneously measured two cardiac biomarkers, cholesterol and choline in the same solution where the authors report linear ranges of 30–240 µM, 0.5–4 µM and LoDs of 3.36 µM and 0.08 µM respectively. The authors demonstrated the use of their sensor within the simultaneous measurement of cholesterol and choline within spiked artificial blood with recoveries of 93–103%. The authors exemplified the use of additive manufacturing where they state that the chip can be easily produced within a medical setting. The method offers specialized and low-cost devices on-demand in the time of need, achieving sensitive bioassays using very simple workflows and short analysis, and it is free from cross-talk phenomena and interferences.<sup>50</sup>

The works highlighted here are important within the field as they emphasise that additive manufactured electrodes can be modified in similar ways to other commonly used electrodes platforms, such as screen printed or glassy carbon electrodes. It is clear that common coupling chemistry used within the field of electrochemical biosensors such as EDC/NHS coupling also works on these electrodes for the immobilisation of the biological recognition elements. Additionally, these works offer an insight into the wide array of designs capable of being produced quickly and simply using FFF technology. Although these works show advantages of additive manufacturing toward the generation of biosensors, the electroanalytical performances are typically not impressive, being hindered by the electrode material. The conductivity values obtained by these commercial filaments are significantly lower than those seen using alternative common electrodes. Therefore, once immobilised with further reagents that hinder electron transfer at the electrode surface, the sensitivities that can be achieved are found to be inadequate. To improve these sensors and make them viable for use within the field of commercial biosensors improvements in filament conductivity are required. With a lack of improvements seen in the marketplace, research teams are now turning to the production of their own bespoke filament with increased loadings and combinations of conductive fillers. Next, we turn



to the use of additive manufacturing biosensors using bespoke filaments.

### 3. Additive manufacturing biosensors using bespoke filaments

The ability to make bespoke filaments has received significant attention, where one can vary the thermoplastic, for example into recycled versions, and one can change the conducting components and increase their amount, alongside the use of bio-based plasticizers.<sup>11,33–35,70</sup> The approach to fabricate bespoke filament is summarized within Fig. 3, where two approaches have been developed, one that produces conductive composites using solvent-based methods, and another that employs thermal procedures. The solvent methodology involves a lower startup cost and can be more accessible to lower income research groups, whereas the thermal method is the more environmentally friendly and quicker option, however both can result in highly reproducible filaments.

As shown within Fig. 3B, the authors used a bespoke nanocarbon black (28.5 wt%) within PLA (71.5 wt%) for the detection of SARS-CoV-2 spike S1 protein.<sup>61</sup> Due to the unique nature of this bespoke filament, where the conductive component is higher than that provided from commercial filaments, there was no-need to deviate to chemical and electrochemical

activation. Furthermore, the authors kept the connection length of the electrodes to 2 cm, where it has been reported that in the case of additively manufactured electrodes, the shorter the connection length of the sensors, the lower the charge transfer resistance and improvements in the electrochemical properties can be obtained.<sup>71</sup> The authors used EDC/NHS modification to attach the antibody and they report a linear range of 0.01 to 4.5 nM with a LoD of 2.7 pM for the detection of the S1 spike protein. The authors demonstrated the use of their sensor within human serum and synthetic saliva, where they spiked it with 0.05, 0.1 and 1.0 nM and reported recoveries of 92–105%. Of note, in comparison to those who have used additive manufacturing for the measurement of COVID-19, this reports the lowest LoD and a high sensitivity of 7.6  $\mu\text{A nM}$  due to the use of the bespoke filament which has more active (nanocarbon black) component.

A notable approach has overcome the limitations of having to use electrochemical pretreatment to induce carboxylated groups upon their electrode material by incorporating them into the filament. Kalinke and co-workers<sup>60</sup> show this through the production of a bespoke filament that contains carboxylated multi-walled carbon nanotubes (COOH-MWCNTs) (10 wt%), nanocarbon black (15 wt%), and polyethylene succinate (10 wt%) within recycled PLA (65 wt%); see Fig. 3C. The use of carboxylated MWCNTs allowed for the enhanced direct

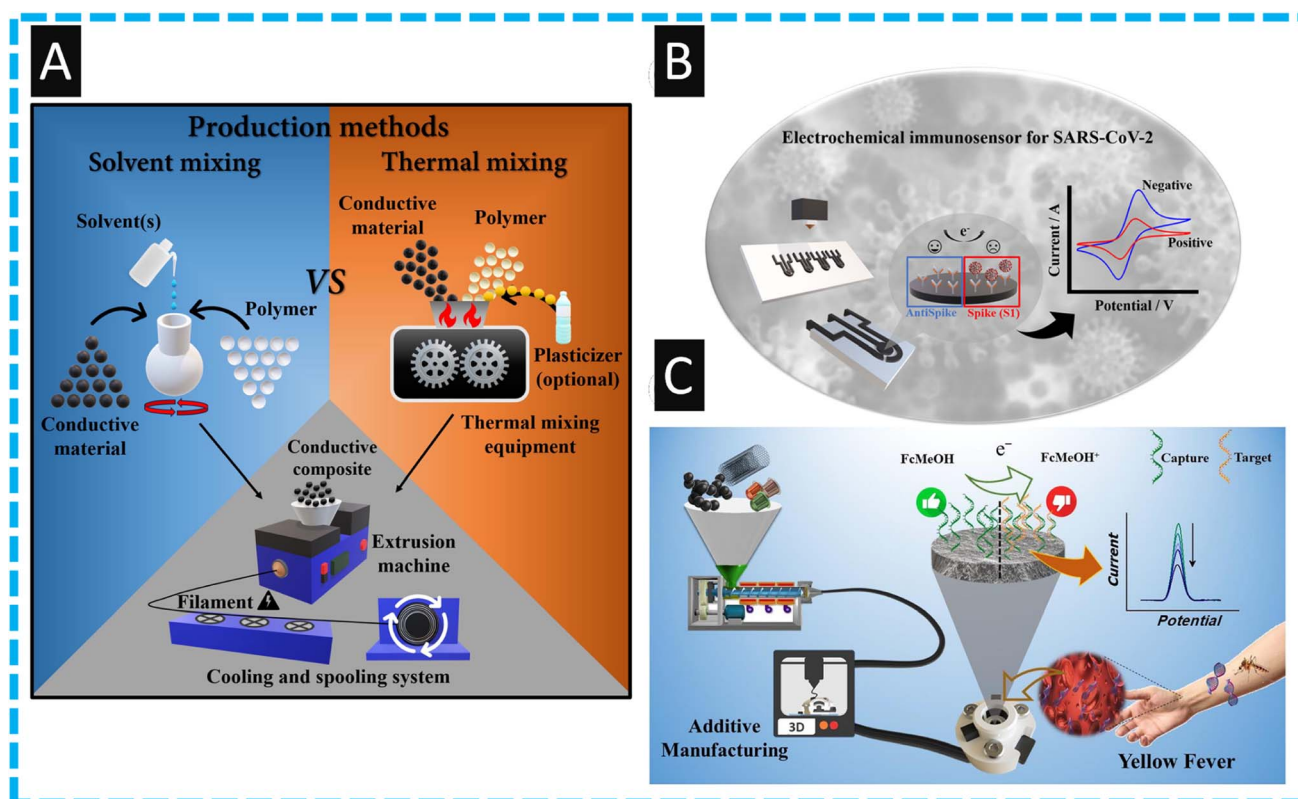


Fig. 3 (A): An overview in the production of conductive composites concerning solvent and thermal approaches and standard method for extrusion and manufacture of conductive filaments. Figure reproduced from ref. 11. Copyright 2023 Elsevier. (B): An overview of the detection of SARS-CoV-2 spike S1 protein using a FFF printed electrode modified with antibodies. Figure reproduced from ref. 61. Copyright 2023 Elsevier; (C): an overview of recycled additive manufacturing feedstocks using carboxylated multi-walled carbon nanotubes as the use as a sensor for yellow fever virus cDNA. Figure reproduced from ref. 60. Copyright 2023 Elsevier.





coupling of the biorecognition element for the preparation of an electrochemical genosensor toward the detection of yellow fever virus cDNA. The authors fabricated their sensor within a bespoke recycled cell using non-conductive recycled PLA and modified their working electrode with the DNA capture probe using the EDS/NHS approach. This allowed the sensing of yellow fever virus cDNA over the range of 0.5 to 15  $\mu\text{M}$ , with a LoD of 0.138  $\mu\text{M}$  which is competitive compared to other electrochemical approaches.<sup>60</sup> The authors demonstrated the use of their sensor within human blood serum reporting recoveries over the range of 95–105% with relative standard deviations of less than 5%. Such an approach allows the design of these devices with the additive manufacturing to be produced on-site, where needed most. Other approaches have made a nanocarbon black (28.5% wt) within PLA (71.5% wt) made through the solvent methodology.<sup>59</sup> These are printed into “lollipop” type electrodes and then modified through chemical and electrochemical treatment. The authors then modified the surface of their electrode *via* the electrodeposition of Prussian Blue towards the sensing of hydrogen peroxide which is important as this is a product of  $\text{GO}_x$ . Using amperometry, the authors demonstrated that the sensor could measure hydrogen peroxide over the range of 5 to 350  $\mu\text{M}$  with a LoD of 1.03  $\mu\text{M}$ . This sensor was shown to detect hydrogen peroxide within spiked milk after a simple dilution with supporting electrolyte, where recoveries were over the range of 85.2–97.1%. These lower recovery values are attributed to the matrix effects of the milk sample<sup>59</sup> and further work needs to be focused upon the sample pre-treatment.

Even so, it is clear that the use of bespoke filaments is required to produce the required electroanalytical sensitivity within the biosensing field, outside of glucose sensors. We would like to encourage authors to publish their filament conductivities within their biosensing manuscripts when using a bespoke filament, as many miss crucial filament characterization measurements. Based on other reports in the literature for bespoke filaments for other applications, they offer significant improvements compared to the commercial options. For example, the most commonly used commercial filament has a conductivity of  $\sim 0.002 \text{ S m}^{-1}$ , whereas some bespoke filaments have reported a 10 $\times$  improvement in this at  $\sim 0.02 \text{ S m}^{-1}$ .<sup>72</sup> Clearly the majority of work on electrochemical biosensors produced through FFF involves the use of PLA based filaments, which have been seen to have issues with solution ingress,<sup>68</sup> memory effects, and performance post sterilisation.<sup>73</sup> These issues need addressing for additive manufacturing electrochemistry to reach its full potential and we foresee significantly more research being published in this area in the coming years due to the synergy between additive manufacturing, electrochemistry and biosensors.

## 4. Future perspectives

It is interesting to note that the high loadings of nanocarbon obtained through solvent mixing methods did not utilise a plasticizer, whereas the thermal method does. Further work needs to be done to look at the effect these two methodologies

have on the physical properties of the filament in terms of low temperature flexibility and polymer degradation. Additionally, there is a lack of work identifying the mixing and dispersion of conductive filler within filaments using these two methodologies. To form the optimal conductive networks through these insulating thermoplastics for the lowest cost, this fundamental understanding should be explored.

As mentioned above, all of the work published using FFF for the production of electrochemical biosensors to date have utilised PLA as the base polymer. This is due primarily to the availability of conductive PLA commercially, the excellent printing properties it possesses, and its ease of combining with nanocarbon fillers. However, there are clear issues with using this polymer for electrochemical applications such as the ingress of solutions<sup>68</sup> and memory effects.<sup>73</sup> There has been the first publication of conductive recycled PETg recently,<sup>73</sup> which offers significantly different material properties to PLA, including greater chemical resistance and lower water ingress. Although this is the case, this PETg filament does not reach the same levels of conductivity seen for the bespoke PLA filaments reported. We expect to see more exploration into different polymer matrices for conductive FFF filament in the future.

Furthermore, it is important to consider the commercialization opportunities and obstacles for biosensor production through additive manufacturing. There are significant benefits that could be realized through the use of additive manufacturing; these include: the production of bespoke, personalized devices to fit an individual's needs through the unique combination of 3D-scanning and printing; production of biosensors of any design *in situ*, anywhere a 3D-printer can be powered; production of exact amounts of sensors quickly to meet localized demand; and the use of different materials to tailor for individual applications. The exciting thing about these potential benefits are they cater for healthcare across the financial spectrum, where bespoke personalized healthcare items would be sought after and improve healthcare for wealthier clientele. Whereas the ability to print on-demand sensors *in situ*, on a cheap printer out of relatively cheap filament could potentially be revolutionary toward fighting future global outbreaks through testing with current bespoke filaments able to produce electrodes for less than 10 (GBP) pence depending on the size, meaning most of the cost would come from the biological components of the biosensor. To achieve this ideal scenario, many hurdles must be overcome. The application of these bespoke filaments toward biosensing applications, as there are now several bespoke filament compositions reported in the literature but relatively few are aimed toward biosensing, most likely due to the time and monetary constraints of this research. Reliability and reproducibility of these filaments over different batches and biosensor production should be at the forefront of these papers by testing biosensors from different parts of the filament to ensure quality performance. Last, costings and upscaling potential should be considered. Is solvent mixing viable for mass filament production if it requires harsh chemicals and hours of mixing? We believe not. These issues need to be addressed to allow this field to move from interesting research





topics to real-world products and solutions withing the healthcare arsenal.

## 5. Conclusions

We have reviewed the use of fused filament fabrication for the production of electrochemical biosensors. Clearly the use of this additive manufacturing technology allows one to rapidly make the basics of the biosensor, where the process is scalable by being able to print many parts onto one print bed. Additionally, through the use of a print farm, it is economical, allowing on-site printing of customized and bespoke biosensors ready to be used by clinical end-users. We can see that bespoke filaments provide significantly enhanced sensing platforms and research should be focused on expanding their use toward developing new biosensors. It is evident that as the field has progressed, the early pioneers used their additive manufacturing electrode “as is”, but it is well understood that the electrochemical performance can be enhanced by applying chemical and electrochemical treatments. We anticipate that future work will look to move away from PLA toward other printable polymers due to ingress and stability issues. Also, future reports using additive manufacturing biosensors authors should ensure their results are validated against other standard laboratory approaches to encourage their commercialization.

## Author contributions

Writing—original draft preparation, writing—review and editing: R. D. C; conceptualization, writing—original draft preparation, writing—review and editing: C. E. B; all authors have read and agreed to the published version of the manuscript.

## Conflicts of interest

The authors declare no conflict of interest.

## References

- 1 S. Rajesh and A. S. Kumawat, *Ionics*, 2024, **30**, 677–687.
- 2 M. J. Whittingham, R. D. Crapnell, E. J. Rothwell, N. J. Hurst and C. E. Banks, *Talanta Open*, 2021, **4**, 100051.
- 3 A. L. Silva, G. M. d. S. Salvador, S. V. Castro, N. M. Carvalho and R. A. Munoz, *Front. Chem.*, 2021, **9**, 684256.
- 4 H. Agrawaal and J. E. Thompson, *Talanta Open*, 2021, **3**, 100036.
- 5 S. A. M. Tofail, E. P. Koumoulos, A. Bandyopadhyay, S. Bose, L. O'Donoghue and C. Charitidis, *Mater. Today*, 2018, **21**, 22–37.
- 6 I. Gibson, D. W. Rosen, B. Stucker, M. Khorasani, D. Rosen, B. Stucker and M. Khorasani, *Additive Manufacturing Technologies*, Springer, 2021.
- 7 W. Liu, X. Liu, Y. Liu, J. Wang, S. Evans and M. Yang, *Sustainability*, 2023, **15**, 3827.
- 8 S. Ford and M. Despeisse, *J. Cleaner Prod.*, 2016, **137**, 1573–1587.

- 9 Y. Huang, M. C. Leu, J. Mazumder and A. Donmez, *J. Manuf. Sci. Eng.*, 2015, **137**, 014001.
- 10 A. Bandyopadhyay and S. Bose, *Additive Manufacturing*, CRC press, 2019.
- 11 R. D. Crapnell, C. Kalinke, L. R. G. Silva, J. S. Stefano, R. J. Williams, R. A. Abarza Munoz, J. A. Bonacin, B. C. Janegitz and C. E. Banks, *Mater. Today*, 2023, **71**, 73–90.
- 12 M. S. Sumitha and T. S. Xavier, *Hybrid Adv.*, 2023, **2**, 100023.
- 13 A. Singh, A. Sharma, A. Ahmed, A. K. Sundramoorthy, H. Furukawa, S. Arya and A. Khosla, *Biosensors*, 2021, **11**, 336.
- 14 M. Banakar, M. Hamidi, Z. Khurshid, M. S. Zafar, J. Sapkota, R. Azizian and D. Rokaya, *Biosensors*, 2022, **12**, 927.
- 15 S. Madhurantakam, S. Muthukumar and S. Prasad, *ACS Omega*, 2022, **7**, 12467–12473.
- 16 K. Wang, X. Lin, M. Zhang, Y. Li, C. Luo and J. Wu, *Biosensors*, 2022, **12**, 959.
- 17 K. C. Honeychurch and M. Piano, *Biosensors*, 2018, **8**, 57.
- 18 R. D. Crapnell, N. C. Dempsey, E. Sigley, A. Tridente and C. E. Banks, *Microchim. Acta*, 2022, **189**, 142.
- 19 A. G.-M. Ferrari, R. D. Crapnell and C. E. Banks, *Biosensors*, 2021, **11**, 291.
- 20 D. Grieshaber, R. MacKenzie, J. Vörös and E. Reimhult, *Sensors*, 2008, **8**, 1400–1458.
- 21 I.-H. Cho, D. H. Kim and S. Park, *Biomater. Res.*, 2020, **24**, 6.
- 22 A. Yang and F. Yan, *ACS Appl. Electron. Mater.*, 2021, **3**, 53–67.
- 23 M. Patel, M. Agrawal and A. Srivastava, *Mater. Adv.*, 2022, **3**, 8864–8885.
- 24 J. H. Kim, Y. J. Suh, D. Park, H. Yim, H. Kim, H. J. Kim, D. S. Yoon and K. S. Hwang, *Biomed. Eng. Lett.*, 2021, **11**, 309–334.
- 25 R. S. Shergill, P. Bhatia, L. Johnstone and B. A. Patel, *ACS Sustainable Chem. Eng.*, 2024, **12**, 416–422.
- 26 C. Kalinke, N. V. Neumsteir, G. d. O. Aparecido, T. V. d. B. Ferraz, P. L. dos Santos, B. C. Janegitz and J. A. Bonacin, *Analyst*, 2020, **145**, 1207–1218.
- 27 R. S. Shergill, A. Farlow, F. Perez and B. A. Patel, *Microchim. Acta*, 2022, **189**, 100.
- 28 B. Hüner, N. Demir and M. F. Kaya, *Fuel*, 2023, **331**, 125971.
- 29 J. G. Walters, S. Ahmed, I. M. Terrero Rodríguez and G. D. O'Neil, *Electroanalysis*, 2020, **32**, 859–866.
- 30 R. S. Shergill, C. L. Miller and B. A. Patel, *Sci. Rep.*, 2023, **13**, 339.
- 31 P. L. dos Santos, V. Katic, H. C. Loureiro, M. F. dos Santos, D. P. dos Santos, A. L. B. Formiga and J. A. Bonacin, *Sens. Actuators, B*, 2019, **281**, 837–848.
- 32 P. Wuamprakhon, R. D. Crapnell, E. Sigley, N. J. Hurst, R. J. Williams, M. Sawangphruk, E. M. Keefe and C. E. Banks, *Adv. Sustainable Syst.*, 2023, **7**, 2200407.
- 33 I. V. S. Arantes, R. D. Crapnell, M. J. Whittingham, E. Sigley, T. R. L. C. Paixão and C. E. Banks, *ACS Appl. Eng. Mater.*, 2023, **1**, 2397–2406.
- 34 E. Sigley, C. Kalinke, R. D. Crapnell, M. J. Whittingham, R. J. Williams, E. M. Keefe, B. C. Janegitz, J. A. Bonacin and C. E. Banks, *ACS Sustain. Chem. Eng.*, 2023, **11**, 2978–2988.



- 35 R. D. Crapnell, I. V. S. Arantes, M. J. Whittingham, E. Sigley, C. Kalinke, B. C. Janegitz, J. A. Bonacin, T. R. L. C. Paixão and C. E. Banks, *Green Chem.*, 2023, **25**, 5591–5600.
- 36 J. S. Stefano, L. R. Guterres e Silva, R. G. Rocha, L. C. Brazaca, E. M. Richter, R. A. Abarza Muñoz and B. C. Janegitz, *Anal. Chim. Acta*, 2022, **1191**, 339372.
- 37 C. W. Foster, G. Q. Zou, Y. Jiang, M. P. Down, C. M. Liauw, A. Garcia-Miranda Ferrari, X. Ji, G. C. Smith, P. J. Kelly and C. E. Banks, *Batteries Supercaps*, 2019, **2**, 448–453.
- 38 R. D. Crapnell and C. E. Banks, *Microchim. Acta*, 2021, **188**, 1–23.
- 39 J. Muñoz and M. Pumera, *TrAC, Trends Anal. Chem.*, 2020, **128**, 115933.
- 40 G. Palmara, F. Frascella, I. Roppolo, A. Chiappone and A. Chiadò, *Biosens. Bioelectron.*, 2021, **175**, 112849.
- 41 A. A. Paul, A. D. Aladese and R. S. Marks, *Biosensors*, 2024, **14**, 60.
- 42 R. D. Crapnell, N. C. Dempsey-Hibbert, M. Peeters, A. Tridente and C. E. Banks, *Talanta Open*, 2020, **2**, 100018.
- 43 V. Katseli, A. Economou and C. Kokkinos, *Electrochem. Commun.*, 2019, **103**, 100–103.
- 44 C. L. Manzanares-Palenzuela, S. Hermanova, Z. Sofer and M. Pumera, *Nanoscale*, 2019, **11**, 12124–12131.
- 45 R. M. Cardoso, P. R. L. Silva, A. P. Lima, D. P. Rocha, T. C. Oliveira, T. M. do Prado, E. L. Fava, O. Fatibello-Filho, E. M. Richter and R. A. A. Muñoz, *Sens. Actuators, B*, 2020, **307**, 127621.
- 46 V. A. O. P. Silva, W. S. Fernandes-Junior, D. P. Rocha, J. S. Stefano, R. A. A. Munoz, J. A. Bonacin and B. C. Janegitz, *Biosens. Bioelectron.*, 2020, **170**, 112684.
- 47 A. M. López Marzo, C. C. Mayorga-Martinez and M. Pumera, *Biosens. Bioelectron.*, 2020, **151**, 111980.
- 48 J. Muñoz and M. Pumera, *Chem. Eng. J.*, 2021, **425**, 131433.
- 49 F. de Matos Morawski, G. Martins, M. K. Ramos, A. J. G. Zarbin, L. Blanes, M. F. Bergamini and L. H. Marcolino-Junior, *Anal. Chim. Acta*, 2023, **1258**, 341169.
- 50 E. Koukouvi and C. Kokkinos, *Anal. Chim. Acta*, 2021, **1186**, 339114.
- 51 L. Wang and M. Pumera, *Microchim. Acta*, 2021, **188**, 374.
- 52 G. Martins, J. L. Gogola, L. H. Budni, B. C. Janegitz, L. H. Marcolino-Junior and M. F. Bergamini, *Anal. Chim. Acta*, 2021, **1147**, 30–37.
- 53 L. R. G. Silva, J. S. Stefano, L. O. Orzari, L. C. Brazaca, E. Carrilho, L. H. Marcolino-Junior, M. F. Bergamini, R. A. A. Munoz and B. C. Janegitz, *Biosensors*, 2022, **12**, 622.
- 54 M. Angelopoulou, D. Kourti, M. Mertiri, P. Petrou, S. Kakabakos and C. Kokkinos, *Chemosensors*, 2023, **11**, 475.
- 55 M. F. Jyoti, M. Hermanová, H. Pivoňková, O. Alduhaish and M. Pumera, *Electrochem. Commun.*, 2023, **151**, 107508.
- 56 J. Muñoz, J. Oliver-De La Cruz, G. Forte and M. Pumera, *Biosens. Bioelectron.*, 2023, **226**, 115113.
- 57 C. Kalinke, P. R. De Oliveira, C. E. Banks, B. C. Janegitz and J. A. Bonacin, *Sens. Actuators, B*, 2023, **381**, 133353.
- 58 J. Lee, S. Maji and H. Lee, *Biotechnol. J.*, 2023, **18**, 2300154.
- 59 J. S. Stefano, L. R. G. e. Silva and B. C. Janegitz, *Microchim. Acta*, 2022, **189**, 414.
- 60 C. Kalinke, R. D. Crapnell, E. Sigley, M. J. Whittingham, P. R. de Oliveira, L. C. Brazaca, B. C. Janegitz, J. A. Bonacin and C. E. Banks, *Chem. Eng. J.*, 2023, **467**, 143513.
- 61 L. R. G. Silva, J. S. Stefano, R. D. Crapnell, C. E. Banks and B. C. Janegitz, *Talanta Open*, 2023, **8**, 100250.
- 62 G. Rocchitta, A. Spanu, S. Babudieri, G. Latte, G. Madeddu, G. Galleri, S. Nuvoli, P. Bagella, M. I. Demartis, V. Fiore, R. Manetti and P. A. Serra, *Sensors*, 2016, **16**, 780.
- 63 R. D. Crapnell, E. Bernalte, A. G.-M. Ferrari, M. J. Whittingham, R. J. Williams, N. J. Hurst and C. E. Banks, *ACS Meas. Sci. Au*, 2021, **2**, 167–176.
- 64 R. D. Crapnell, E. Sigley, R. J. Williams, T. Brine, A. Garcia-Miranda Ferrari, C. Kalinke, B. C. Janegitz, J. A. Bonacin and C. E. Banks, *ACS Sustainable Chem. Eng.*, 2023, **11**, 9183–9193.
- 65 H. Teymourian, A. Barfidokht and J. Wang, *Chem. Soc. Rev.*, 2020, **49**, 7671–7709.
- 66 L. He, S. Lin, H. Pan, R. Shen, M. Wang, Z. Liu, S. Sun, Y. Tan, Y. Wang and S. Chen, *Front. Aging Neurosci.*, 2019, **11**, 24.
- 67 Z. Hong, M. Shi, K. A. Chung, J. F. Quinn, E. R. Peskind, D. Galasko, J. Jankovic, C. P. Zabetian, J. B. Leverenz and G. Baird, *Brain*, 2010, **133**, 713–726.
- 68 R. J. Williams, T. Brine, R. D. Crapnell, A. G.-M. Ferrari and C. E. Banks, *Mater. Adv.*, 2022, **3**, 7632–7639.
- 69 T. Avšič-Županc, A. Saksida and M. Korva, *Clin. Microbiol. Infect.*, 2019, **21**, e6–e16.
- 70 I. V. Arantes, R. D. Crapnell, E. Bernalte, M. J. Whittingham, T. R. Paixão and C. E. Banks, *Anal. Chem.*, 2023, **95**, 15086–15093.
- 71 R. D. Crapnell, A. Garcia-Miranda Ferrari, M. J. Whittingham, E. Sigley, N. J. Hurst, E. M. Keefe and C. E. Banks, *Sensors*, 2022, **22**, 9521.
- 72 R. D. Crapnell, I. V. Arantes, J. R. Camargo, E. Bernalte, M. J. Whittingham, B. C. Janegitz, T. R. Paixão and C. E. Banks, *Microchim. Acta*, 2024, **191**, 96.
- 73 R. D. Crapnell, E. Bernalte, E. Sigley and C. E. Banks, *RSC Adv.*, 2024, **14**, 8108–8115.

